



Abdallah, S. R., Saidani-Scott, H., & Benedi, J. (2019). Experimental study for thermal regulation of photovoltaic panels using saturated zeolite with water. *Solar Energy*, 188, 464-474.  
<https://doi.org/10.1016/j.solener.2019.06.039>

Peer reviewed version

License (if available):  
CC BY-NC-ND

Link to published version (if available):  
[10.1016/j.solener.2019.06.039](https://doi.org/10.1016/j.solener.2019.06.039)

[Link to publication record in Explore Bristol Research](#)  
PDF-document

This is the author accepted manuscript (AAM). The final published version (version of record) is available online via Elsevier at <https://www.sciencedirect.com/science/article/pii/S0038092X19306140?via%3Dihub>. Please refer to any applicable terms of use of the publisher.

## University of Bristol - Explore Bristol Research

### General rights

This document is made available in accordance with publisher policies. Please cite only the published version using the reference above. Full terms of use are available:  
<http://www.bristol.ac.uk/red/research-policy/pure/user-guides/ebr-terms/>

# Experimental Study for Thermal Regulation of Photovoltaic Panels Using Saturated Zeolite with Water

Saber Ragab Abdallah <sup>1,a,b</sup>, Hind Saidani-Scott <sup>2,a</sup>, Jorge Benedi <sup>3,c</sup>

<sup>1</sup>[Saber.abdo@bristol.ac.uk](mailto:Saber.abdo@bristol.ac.uk), <sup>2</sup>[h.saidani@bristol.ac.uk](mailto:h.saidani@bristol.ac.uk), <sup>3</sup>[jorgebenedi1997@gmail.com](mailto:jorgebenedi1997@gmail.com)

<sup>a</sup> Mechanical Engineering Department, University of Bristol, United Kingdom.

<sup>b</sup> Mechanical Engineering Department, Shoubra Faculty of Engineering, Benha University, Egypt.

<sup>c</sup> School of Engineering Design, Universitat Politècnica de València, Spain.

---

## Abstract

This paper presents a novel experimental work for cooling photovoltaic panels using water saturated zeolite/activated alumina. Different system configurations, with 4 different zeolite thicknesses, were tested indoor. Moreover, the zeolite was tested with different added components (fins and metal mesh/particles) for enhancing the system performance. Three different radiations intensities were set for a period of 6 hours and the results were compared with the uncooled system. The experimental results showed a significant solar panels temperature reduction of approximately 14.9°C and 9 °C for radiation intensities of 600 and 1000 W/m<sup>2</sup> respectively. The expected electrical efficiency, according to this temperature reduction, was calculated and an average enhancement of 10% and 7% at radiation of 600 and 1000 W/m<sup>2</sup> intensity respectively was estimated.

**Key words: Solar panels, cooling, materials, Zeolite, saturated**

---

## 1. Introduction

Technology development, luxury and comfort living plus the increase population are some of the reasons that lead to higher energy demand and consumption. According to latest statistical review of world energy in June 2018 [1], power generation increased by 2.8% because of emerging economics and the share of renewable energy in world power consumption reached 8.4%. Due to the impact of this consumption increase on the environment and decaying of the fuel resources, the world trended to shift to more dependence on renewable energy resources. Solar energy, wind energy, and hydro energy are the most developed types of renewable energies. Producing useful energy from solar energy (either heat or electricity) was and still a big issue to deal with due to low energy conversion efficiency. Solar panels have been studied by many researchers and scientists for the last three decades. Their work focussed on PV panel's material for efficiency improvement [2,3] and reached an average efficiency for the commercial panels of 18% [4]. From another perspective, rather than improving the PV material itself, other team of researchers worked on improving the performance of solar panels by controlling the panel temperature which can lead to the reduction of power loss and efficiency degradation, consequently increasing the conversion efficiency from 10 to 25% - depending on the installation location [5].

Many trials were implemented to thermally regulate solar panels temperature. From the heat transfer point of view, these trials are classified into two main categories: Active and passive systems. Active systems are systems that use energy to run external pump, blower or fan to force the flow over solar panels (based on forced convection). The passive system is based on attaching a stagnant medium over either the back or front surface of the PV panel [6].

For active systems, many cooling mediums (fluids) are used, including air, water and Nanofluids. Convective air systems [7] contain blower over the back and/or front surface of PV panels, with different air velocities, different cooling channels and different fins arrangements. However, convective water systems, in either open or closed loops, use different cooling coil configurations on the back surface of the panel with different flow rates and different end usage for the heated water [8,9]. On the other hand, Nanofluids convective systems are using different types of Nano materials, again with different flow rates, different concentrations and combinations of different types of Nano particles [10-12].

For the passive system, many experiments were done based on either buoyancy force or phase change processes e.g. ‘liquid-vapour interface in heat pipes’ and solid ‘liquid interface’. They are frequently placed in a container, firmly attached to the rear side of the panel [13-17]. For PCMs (phase change materials), the commonly used material is paraffin wax (RT) with different melting points, depending on various atmospheric temperatures. Moreover, different system configurations were studied using fins, metal mesh and Nano substance additives for improving the thermal characteristics of the PCMs. For liquid-vapour interface, heat pipes technologies were implemented in limited types or researches for studying different filling ratios, finned and un-finned condenser section and different working mediums [18]. Figure 1 shows thermal regulation techniques used for solar panels.

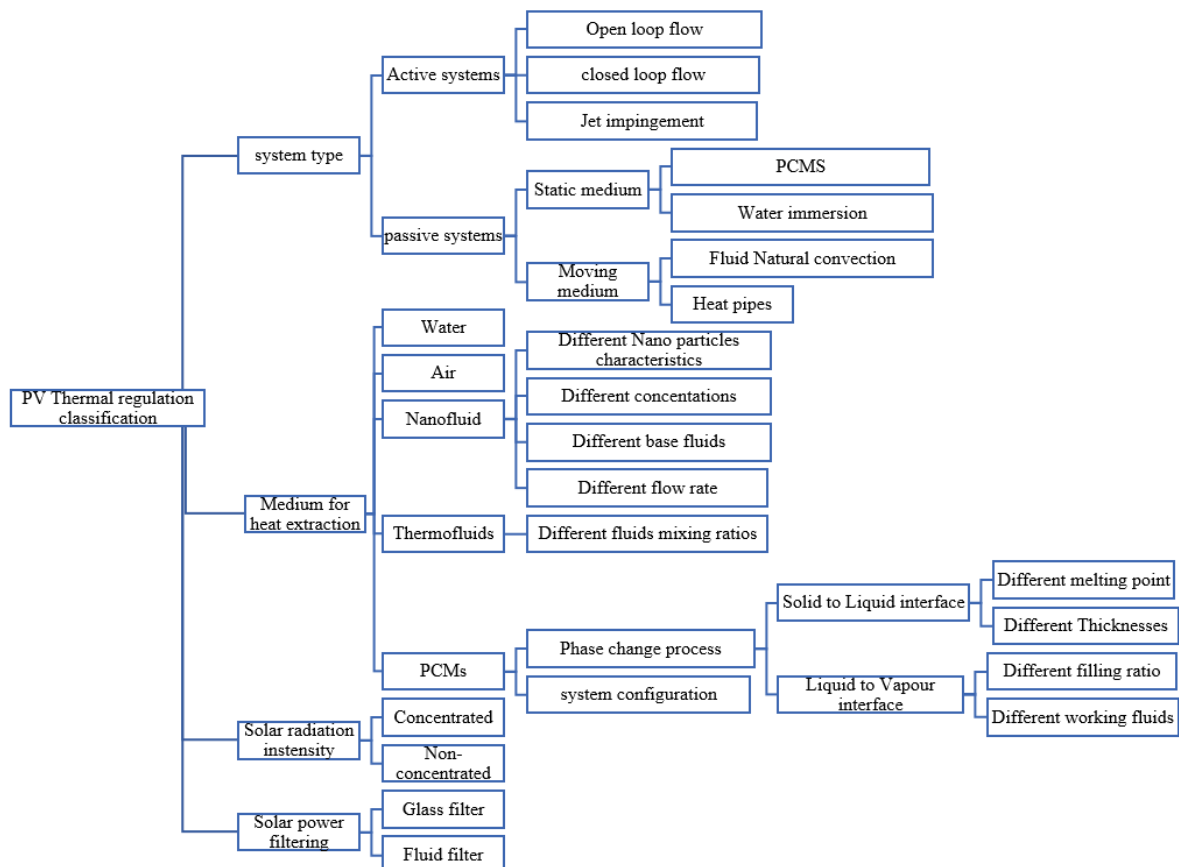


Figure 1: Classification of different thermal regulation techniques used for PV panels.

Another related investigation for regulating solar panel temperature, wind induced convection phenomenon with different wind speeds was used; wind channels beneath the PV and panel orientation versus the coming wind were also investigated in related articles [19-20].

The active systems showed a very powerful heat removal effect; however, the energy consumption to drive the forcing mean is an issue under concern.

Searching for new materials and new system configuration are still a very interesting and challenging field of research. To achieve effective passive cooling, the attached substance should fulfil important characteristics: high thermal conductivity, high specific heat and high latent heat. Water is one of the most available cheap substances, either as pure or sea water. It also has a relatively good thermal characteristics to be an effective cooling medium [21]. Substances which adsorb water at normal atmospheric temperature and desorb it as a form of vapour with heat application are also available commercially and in nature at relatively low cost compared with paraffin wax. There are many different materials of these substances like Silica gel, zeolite, ...etc.

It can be mentioned that, this type of systems' influencing water absorption was only used as desiccant evaporative cooler, controlling rooms and museums temperature and humidity [23] but not yet used for controlling photovoltaic panels temperature. This work aims to present a novel experimental work on thermal regulation of solar panels located in moderate climate countries with temperature range (25-35) °C using zeolite (Activated alumina).

Zeolite is amongst the promising water absorptive substances. It is an adsorbent material that allows the water to go into the pores of their inner particles and not allowing it to leak or evaporate without considerable heating effect. It can also adsorb water up to 15% of its weight in normal atmospheric temperature and allows it to evaporate when temperature raises [22]. Furthermore, zeolite can be manufactured at a low cost or available in nature (like in Japan).

The working principle of the proposed system is to use the porosity and water adsorption properties of zeolite to cool down the PV panels. The gaps between the zeolite particles allow a natural circulation and the heat capacity of water contribute to the PV thermal regulation for longer period. After acquiring enough heat, the zeolite starts to desorb the water in form of water vapour, carrying out the heat from the back surface of the panel. Figure 2 represent a schematic diagram of the proposed thermal regulation process using water absorptive substance.

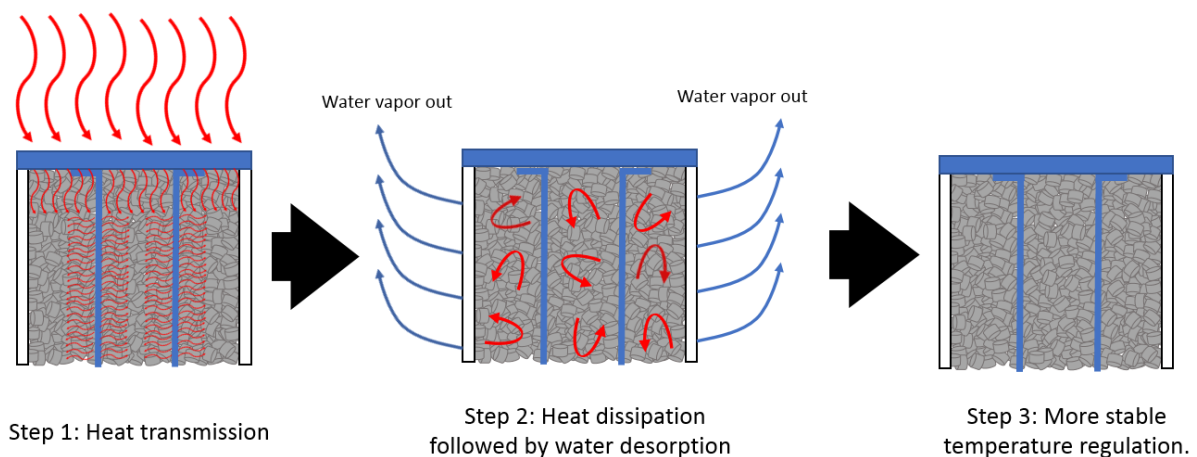


Figure 2: A schematic diagram of the proposed thermal regulation process

A test rig was setup and calibrated in order to evaluate the thermal performance of solar panels under different arrangement of the zeolite. Solar panels were simulated using three blue coated copper plates of emissivity 90% of similar characteristics of PV panels based on experimental results [24], [25].

Only heat transmitted ( $Q$  transmitted in flow chart below, not the total solar energy input to the panel) is considered to be removed at solar radiation of 600, 800 and 1000 W/m<sup>2</sup>. The required radiation was calculated based on figure 3 that represents the heat balance of the system. These radiations were chosen to simulate the minimum, medium and maximum solar radiation that been recorded in outdoor test experiments in [8]. Equation 1 and 2 describe how the incident radiation to the system was calculated to simulate the transmitted heat to the system.

$$Q_{trans.} = I_{total} - E_{generated} \quad \text{Eqn.1}$$

$$E_{gnereated} = I''_{total} * A_s * \eta_{electric} \quad \text{Eqn.2}$$

Where:

$Q_{trans.}$ : Transmitted heat to be removed = actual input to the system W

$I_{total}$ : Total radiation input to PV panels W

$E_{generated}$ : estimated electrical energy output from PV panels W

$I''_{total}$ : total radiation flux into the PV panel W/m<sup>2</sup>

$A_s$ : Solar panel area m<sup>2</sup>

$\eta_{electric}$ : Estimated electrical efficiency based on operating temperature

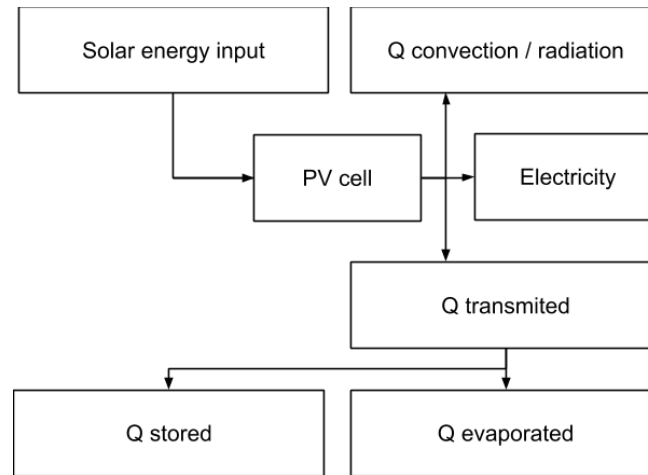


Figure 3: Heat balance of the proposed system

Initially, a 10 cm depth water-saturated zeolite was tested at 1000 W/m<sup>2</sup> and compared to the uncooled system. Fins were then inserted and tested against un-finned system and the reference system. Afterwards, metal mesh cuts/particles were mixed with zeolite to enhance the thermal conductivity of the system then compared with the one without additions of mesh at different radiations. Finally, the effect of different depths of 10, 7.5, 5 and 2.5 cm was studied at different radiations.

## 2. Experimental Setup

Experiments were done at the Thermofluid Laboratory at the University of Bristol uk. The solar light was simulated using a 6x 1kW halogen lamps solar simulator which was assembled over a metal frame with controllable elevation. The halogen lamps were selected to

simulate the solar radiation due to their comparable wavelengths to the solar radiation as shown in figure 4 [26].

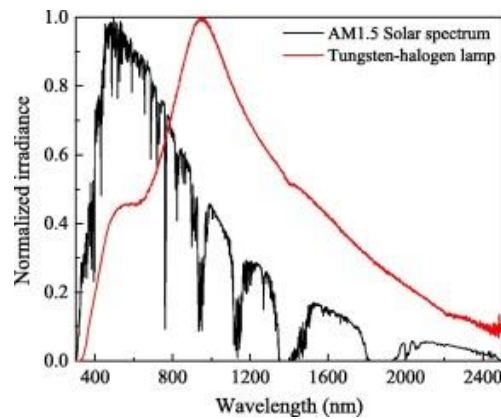


Figure 4: Normalised spectral irradiance for the halogen lamp versus solar intensity AM1.5 [26].

The radiation intensity was calibrated with lamps positioning in order to get three uniform solar radiations of 600, 800 and 1000 W/m<sup>2</sup> for the experimental test purpose. The environmental/surrounding temperature was controlled using air ventilation system over the test time.

Zeolite (Activated alumina tablets) with 7 mm diameter and 5 mm depths were selected and used due to its porosity which can allow the water vapour to escape during the desorption process as shown in figure 5



Figure 5: Activated Alumina used in the experiment.

Three perforated open top boxes of dimensions (15cm length x15cm width x10 cm depth) were made of 6 mm acrylic material as shown in figure 4. Another three perforated boxes with (15 cm length and 15 cm width) but with different depths of 7.5, 5 and 2.5 cm depths to study the effect of the zeolite depth and quantity were used.

Temperatures inside the 10 cm depth boxes were measured using 9 K-type thermocouples for each box. These thermocouples were arrayed at different depths from the upper surface as shown in figure 6. Additionally, two K-type thermocouples were attached to the back surface of the simulating plate. Five data loggers of 8 points each were used to record the temperature every minute. All of the data loggers were connected to a core i7 desktop to store these data on Excel worksheets.



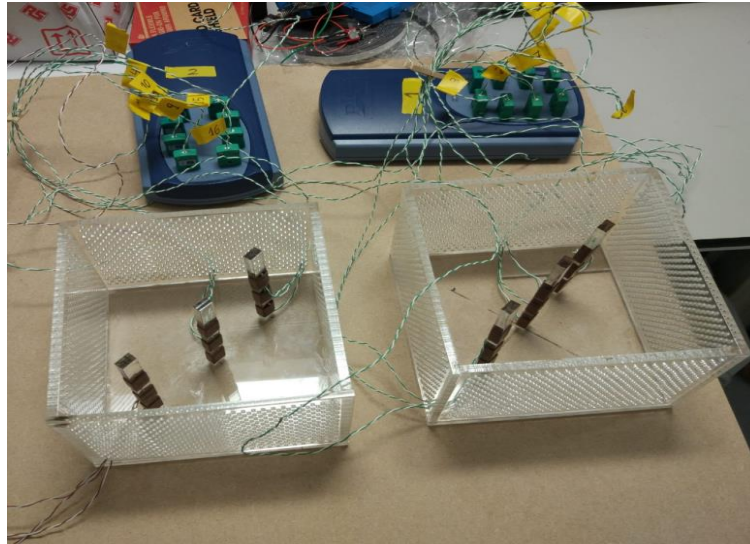


Figure 6: Thermocouples settings inside the boxes.

The complete test rig is shown in figure 7 below, where the three boxes are at different system configuration; the separated painted plate simulate the un-cooled system and the white slab is used to measure the surrounding temperature in shadow below it-inside the test area.

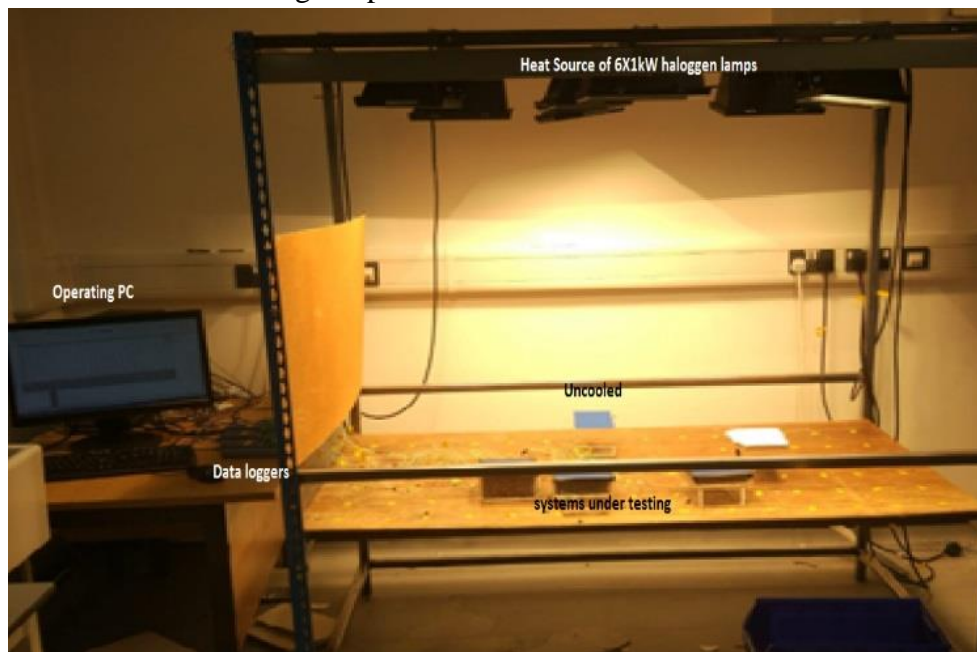


Figure 7: Complete test rig.

To reduce the gap between the copper plates and the zeolite, thin aluminium layers were pushed between the copper plates and the zeolite under pressure as shown in figure 8 below.



Figure 8: Filled boxes before assembling

Figure 9 represents a schematic diagram of the proposed system with various enhancements presented in the study .

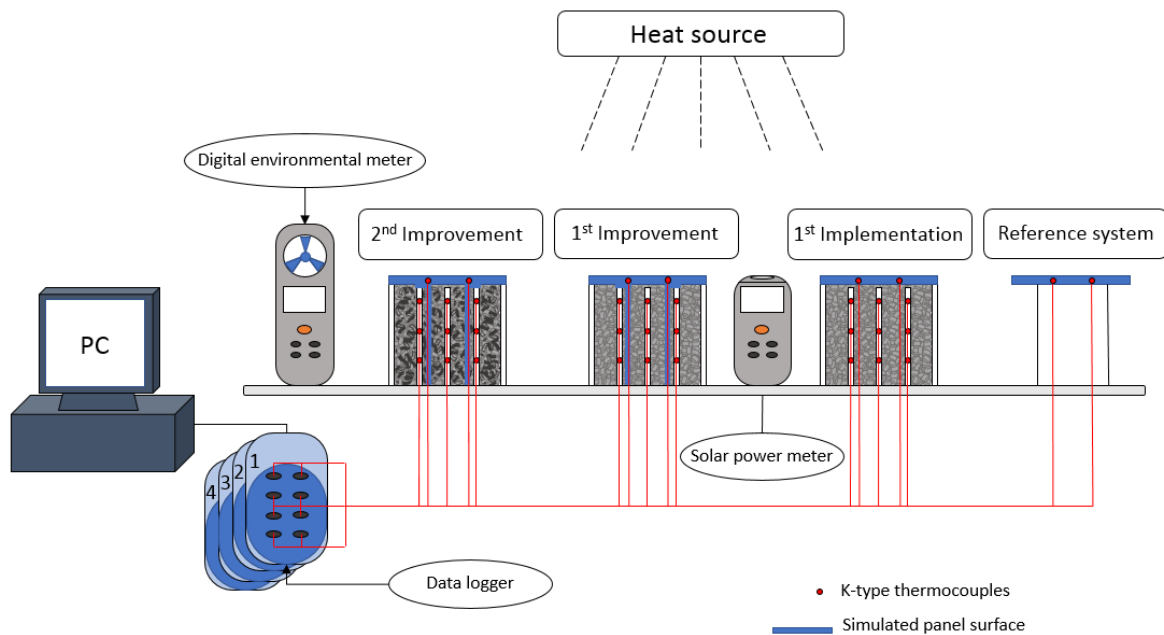


Figure 9: Schematic diagram of the test rig.

A Solar power meter was used to measure the radiation intensity at test locations, and a digital environmental meter was used to monitor the air velocity, ambient temperature and relative humidity at the same level of the test specimens. 38 K type thermocouples were calibrated before the experiment. The specifications of the used instruments for the experiment are shown in table1.

Table 1: Specification of measuring devices

Thermocouples	Type	K-Type
	Range	0 to 275 °C
Weight scale	Range	0 to 4 kg
	Accuracy	±10 g



Thermographic camera	Type	Flir E6
	Range	-20 to 250 °C
	Accuracy	$\pm 2$ %
Data Acquisition system	Type	Pico Technology TC-08
	Accuracy	$\pm 0.2$ %
	Range	-270 to 1370 °C
Solar power meter	Type	Extech SP505
	Range	0 to 3999 W/m <sup>2</sup>
	Accuracy	$\pm 10$ W/m <sup>2</sup>

Zeolite was saturated with water by submersing it for 8 hours before starting experiments and boxes weights were measured before and after each experiment for water loss evaluation. After experiments, the recorded temperatures were used for calculating the expected electrical efficiency using Evans and Florschuetz equation which relates the PV panel efficiency with its temperature [27] as shown in equation 3 below:

$$\eta_{elec.} = \eta_{T_{ref}} [1 - \beta_{ref} (T_{panel} - T_{ref})] \quad \text{Eqn.3}$$

Where,  $\eta_{T_{ref}}$  is the standard efficiency of photovoltaic panel at Standard Test Conditions (STC) and it was taken as 17% based on Trina solar multi-crystalline PV panel data sheets (ALLMAX- PD05.08). Temperature coefficient  $\beta_{ref}$  is also taken as 0.0045 C<sup>-1</sup> for silicon PV panels based on [27],  $T_{ref}$  is the standard test temperature which is 25 °C.

### 3. Experimental Procedures

Experiments were carried out to study the effect of different system parameters: different radiation intensities and different system configurations (e.g. Zeolite depth, Fins insertion, Metal mesh cuts additives). Firstly, the radiation in the test area was measured and calibrated using a calibrated solar power meter. Afterwards, experiments were carried out using a box full of saturated zeolite at 1000 W/m<sup>2</sup> solar radiation and a reference system “un-cooled plate” at the same metrological conditions. Then two rectangle copper fins of the same internal box dimensions were centred and attached to the main plate to enhance the heat transfer rate to the bottom layers of zeolite and compared with the un-finned system and the reference one. Lastly, the finned system was tested under three different solar radiation of 600, 800 and 1000 W/m<sup>2</sup>.

These experiments were followed by inserting Aluminium metal mesh cuts/particles within the wet zeolite to enhance the thermal conductivity through the air gaps and zeolite itself. This was compared with the finned and the reference systems at the same radiation intensities. Finally, different depths of zeolite were tested and compared at 600 and at 800 W/m<sup>2</sup> to optimise the depth of zeolite. All of the experiments were held for 6 continuous hours. The operating temperatures of different systems were used in Evan’s equation and compared with the reference systems. In order to have a clear view of the temperature distribution and contours in the zeolite, a thermographic camera was used.

### 4. Experimental errors and uncertainty

All the instruments used were calibrated and uncertainty analysis was done for all equipment and sensors, including K type thermocouples, solar power meter, weight scale, and thermographic camera. The uncertainty of measurements was calculated using Equation 4 [28].

$$e_r = \left[ \left( \frac{\partial R}{\partial V_1} e_1 \right)^2 + \left( \frac{\partial R}{\partial V_2} e_2 \right)^2 + \dots + \left( \frac{\partial R}{\partial V_n} e_n \right)^2 \right]^{0.5} \quad \text{Eqn.4}$$

From table 1, the uncertainty was calculated as follow

$$e_R = [(0.5)^2 + (0.05)^2 + (0.02)^2 + (0.002)^2 + (0.041)^2]^{0.5} = \pm 0.50$$

The uncertainty value obtained is less than the permissible value for engineering research purposes which is 5%.

## 5. Results and Discussion

To investigate the effect of using water saturated zeolite as a coolant for the solar panels, one system of 10 cm depth wet zeolite was tested versus a reference system under 1000 W/m<sup>2</sup> solar radiation and 30° C +/- 5 °C ambient temperature.

The temperature variation was recorded and plotted over 6 hours of the experiment as shown in figure 10. From the figure, it can be noticed that the temperature of the reference system ( in blue) has a significant sharp increase in the first 15 min and stabilised after. For the wet zeolite system, the temperature had less sharp increase initially and maintain the surface temperature of the cooled system below the reference system for 3 hours.

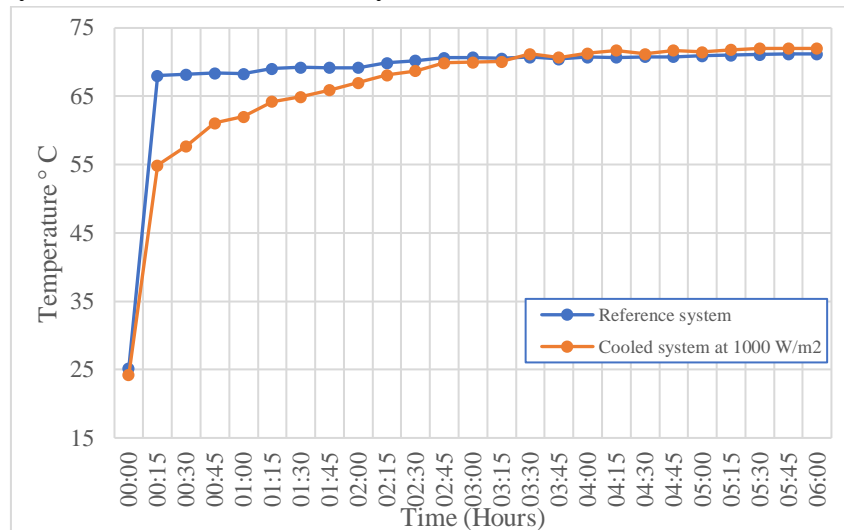


Figure 10: Temperature for wet zeolite system versus the reference system at 1000 W/m<sup>2</sup> solar radiation

This temperature reduction occurred because of the capability of wet zeolite to absorb some of the excess heat. This temperature regulation was reflected positively on the calculated expected electrical efficiency from Evan's equation as shown in figure 11.

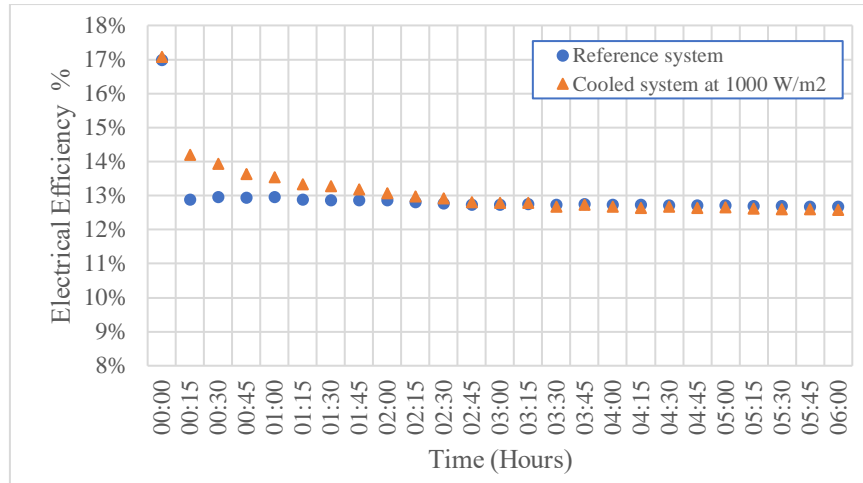


Figure 11: Electrical efficiency for wet zeolite system and the reference system at 1000 W/m<sup>2</sup> solar radiation.

The system showed an acceptable cooling performance for 3 hours only because the heat was transmitted through the first 2 centimetres of zeolite and didn't reach the lower layers due to the low thermal conductivity of zeolite and the air gaps between its particles as shown in the side view thermographic image (figure 12) below. It is obvious from the image that the heat wasn't fairly transmitted through the zeolite layers apart from the first 2 centimetres depth, hence the temperature increased with time approaching that of the uncooled one.

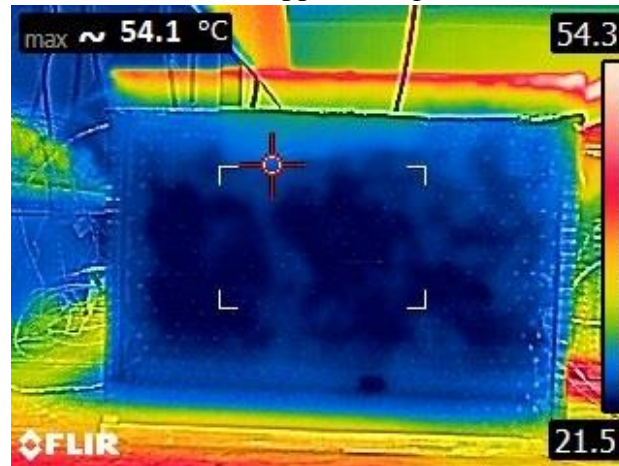


Figure 12: Thermo graphical image (Side view) for the temperature distribution through the zeolite.

In order to improve the heat transfer to the bottom layers of the zeolite, two copper fins (10 cm depth, 1 mm thickness and 5 cm apart) were attached to the back surface of the plate. This addition of the fins enhanced the heat transfer to the bottom layers and increased the thermal performance of the whole system. With this new system configuration (Wet zeolite with 10 cm depth + 2 fins), three experiments were held and repeated with three different radiations (600, 800 and 1000) W/m<sup>2</sup>.

Figures 13.a, 13.b and 13.c represent the temperature difference between the cooled system with fins and the reference at 600, 800, and 1000 W/m<sup>2</sup> solar radiation respectively. From the figures, it can be noted that the system performance with inserting metal fins showed better

results than un-finned one as it maintained more reduction in temperature between the cooled system and the reference for the 6 hours of the experiment. The maximum temperature difference was found at 600 W/m<sup>2</sup> solar radiation while fins were able to dissipate the heat to the other layers and reduce the panel temperature.

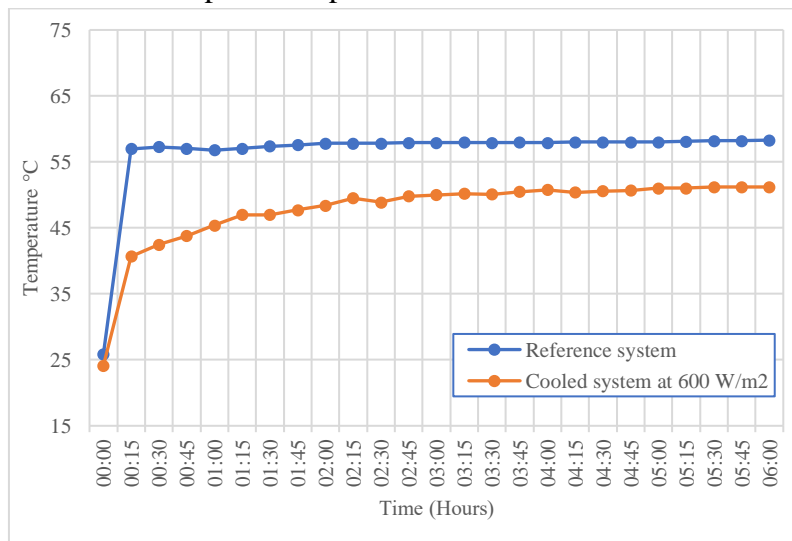


Figure 13.a

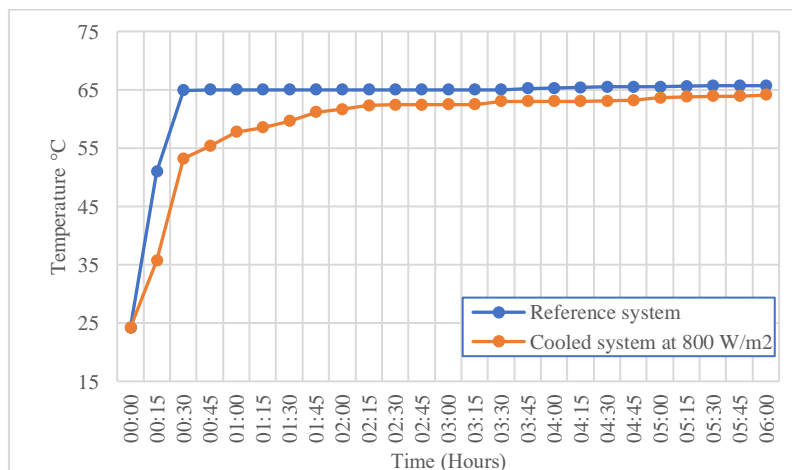


Figure 13.b

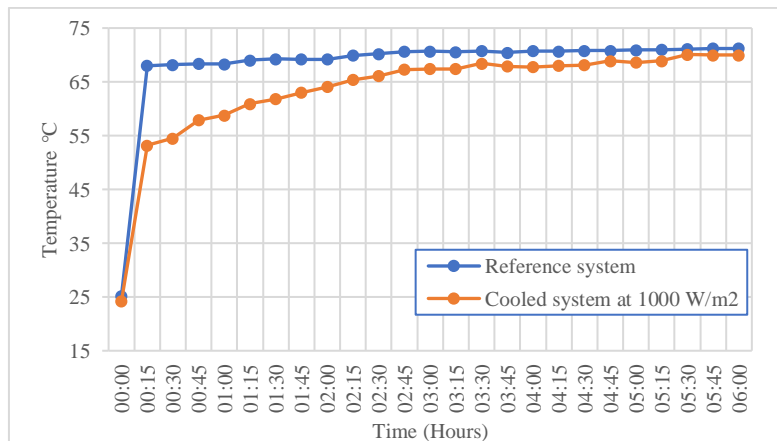


Figure 13.c

Figure 13: Cooled panel temperature using fins versus reference panel at a. 600 W/m<sup>2</sup>, b. 800 W/m<sup>2</sup> and c. 1000 W/m<sup>2</sup> radiation.

Figures 14.a, 14.b and 14.c represent the expected calculated electrical efficiency for different radiation intensities. The efficiency graphs showed a good reflection for the effect of adding fins for enhancing the cooling performance.

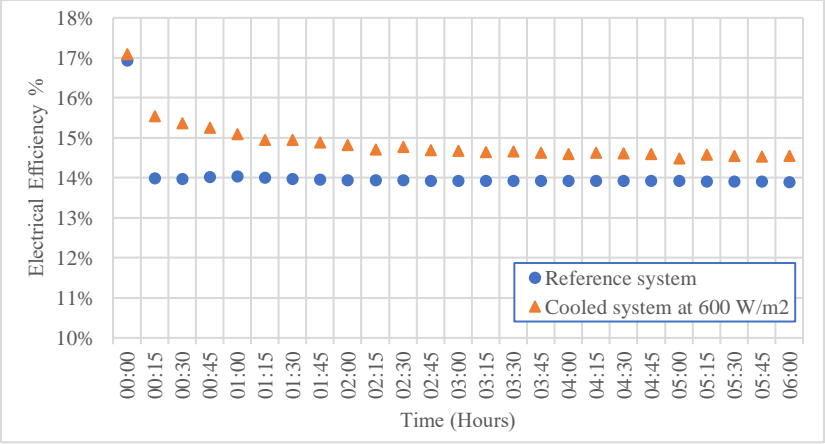


Figure 14.a

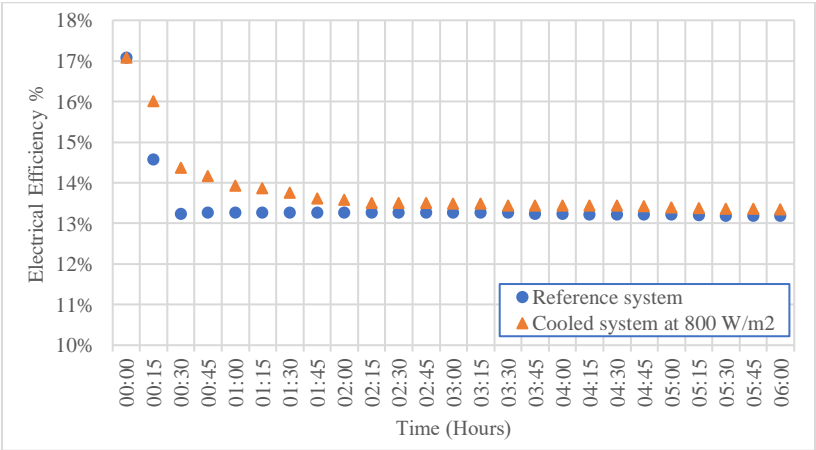


Figure 14.b

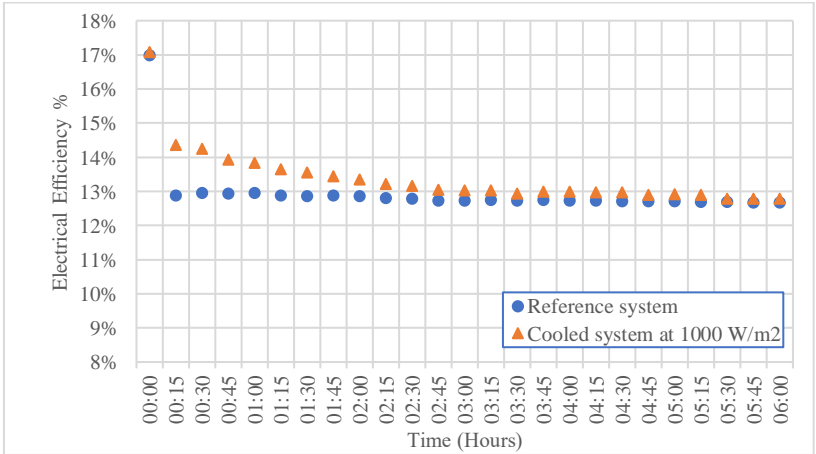


Figure 14.c

Figure 14: Cooled panel electrical efficiency variation using fins versus reference panel at 600 W/m<sup>2</sup>, b. 800 W/m<sup>2</sup> and c. 1000 W/m<sup>2</sup> radiation.

When increasing the radiation, the performance was good but need to have better improvements to maintain more heat regulation for higher radiations which led the experiment to the third phase. The third phase of the experiment was to mix Aluminium mesh cuts/ particles (1% of the total weight) with the zeolite parallel with fins to enhance the thermal conductivity of the overall system. Experiments were performed at three different radiations (600, 800 and 1000) W/m<sup>2</sup> and compared with the reference system and the finned system only. Figures 15.a, 15.b and 15.c shows the variation of the temperature of the three system configurations under different radiations. From these figures it can be noted that, adding aluminium mesh cuts with only 1% of the total weight increased the overall system performance. This significant effect is due to increasing thermal conductivity of the medium and to filling the air gaps between zeolite tablets.

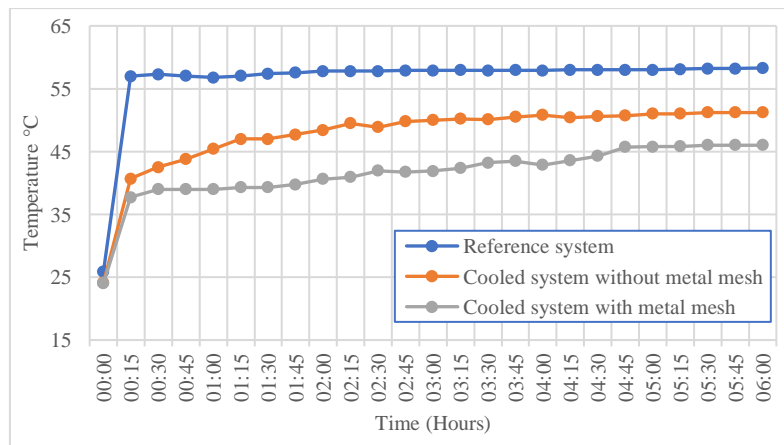


Figure 15.a

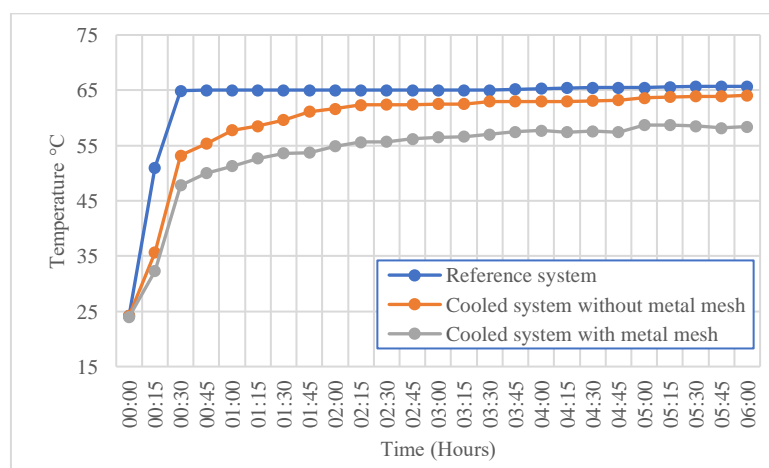


Figure 15.b



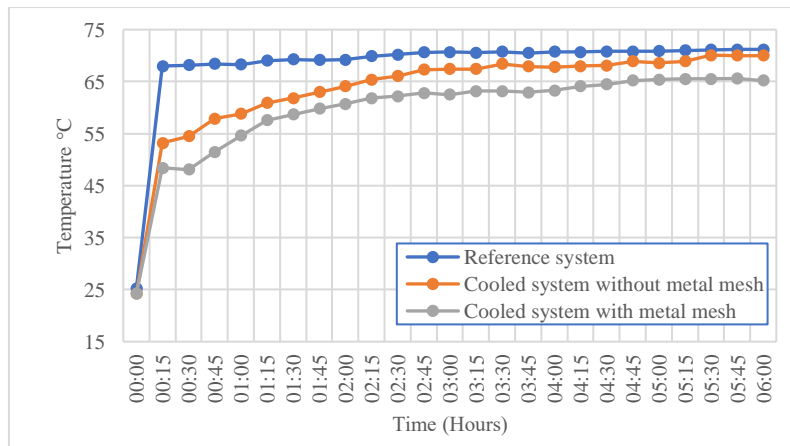


Figure 15.c

Figure 15: Cooled panel temperature variation using fins and metal mesh versus fins only and reference panel at a. 600 W/m<sup>2</sup>, b. 800 W/m<sup>2</sup> and c. 1000 W/m<sup>2</sup> radiation.

Moving more heat caused more desorption of water hence reduction of heat storage inside the wet zeolite itself consequently reducing panel temperature. The expected electrical efficiencies from these systems under different radiations are shown in figures 16.a, 16.b and 16.c.

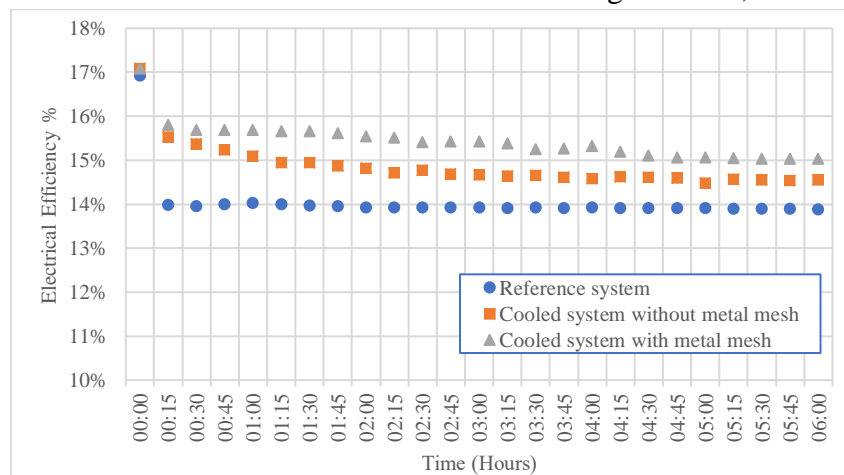


Figure 16.a

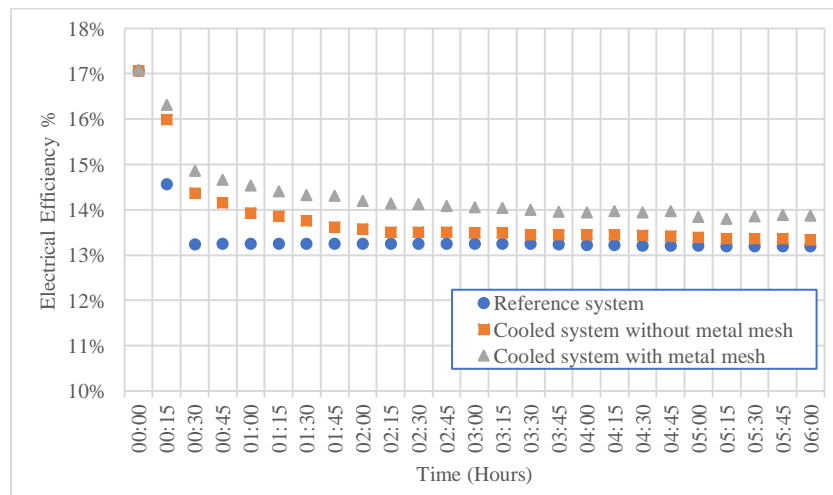


Figure 16.b

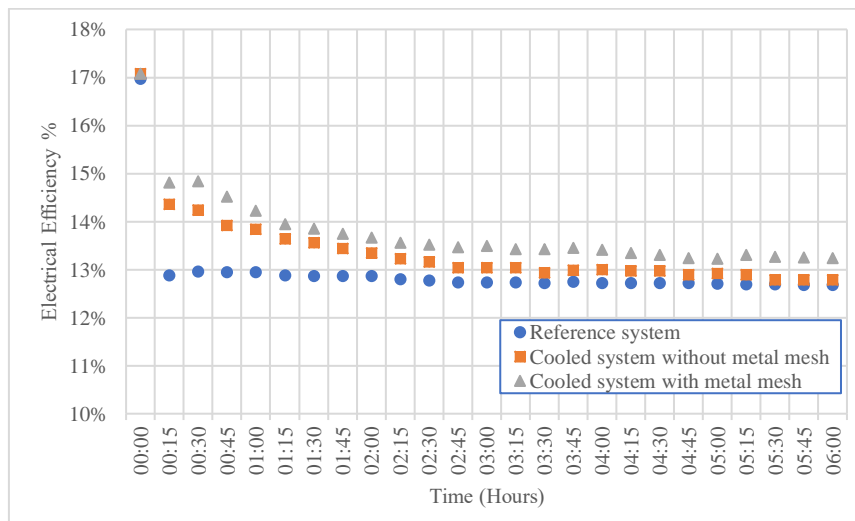


Figure 16.c

Figure 16: Cooled panel electrical efficiency using fins metal fins and mesh versus fins only and reference panel at a.  $600 \text{ W/m}^2$ , b.  $800 \text{ W/m}^2$  and c.  $1000 \text{ W/m}^2$  radiation.

Figure 17 represents a side view temperature distribution within the system zeolite/metal mesh/fins insertion with a thermographic camera. From this graph, it can be noticed that the heat is widely dissipated through the whole system and reached up to the bottom layer of zeolite because of adding both fins and metal mesh cuts as well.

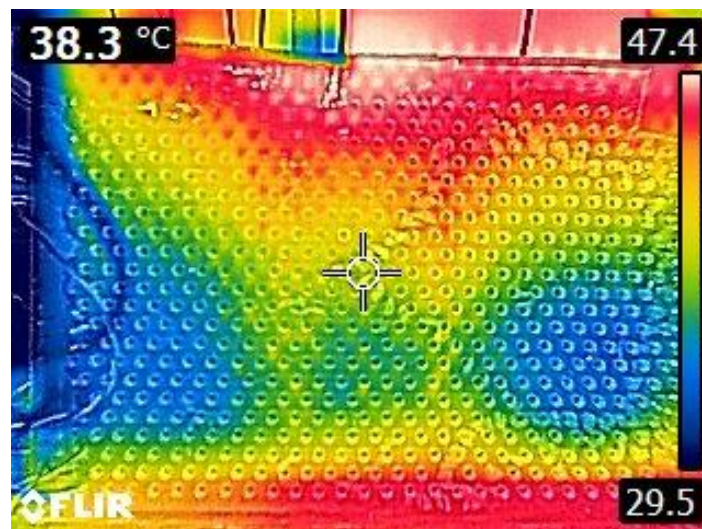


Figure 17: Temperature distribution among the system using both fins and metal mesh cuts.

To study the effect of zeolite depth on the system performance, four different depths of (10, 7.5, 5 and 2.5 ) cm were tested and compared at 600 and 800W/m<sup>2</sup>. Figures 18.a and 18.b show the temperature variation over 6 hours for different depths at different radiations. It is noticeably seen that increasing the depth of the wet zeolite increases the system cooling performance. This is because reducing the depth/thickness of wet Zeolite decreases the ability

of the system to acquire or store the incident heat and even becomes worse than the reference system which is exposed to the convection from both sides.

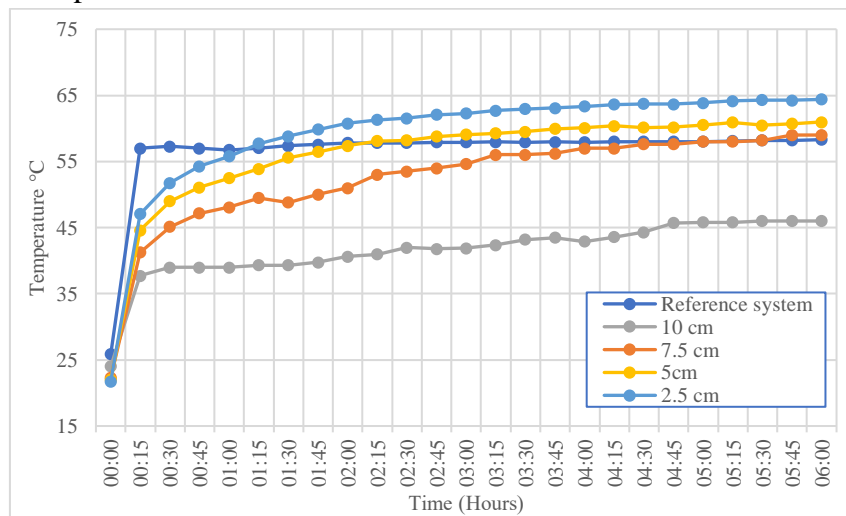


Figure 18.a

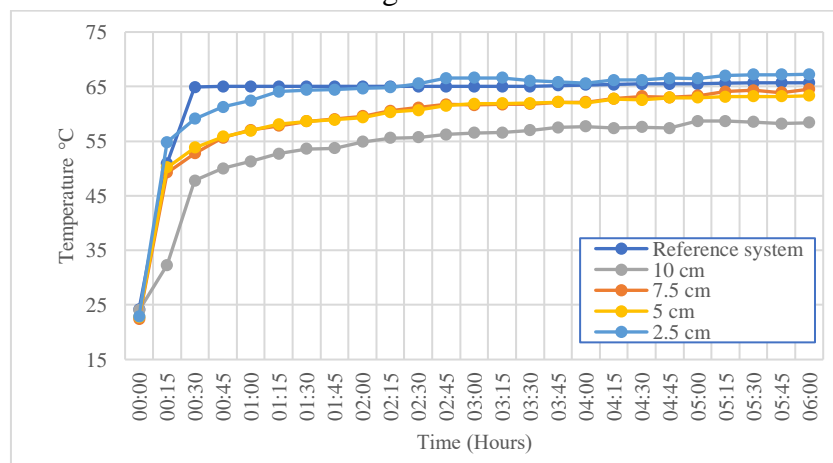


Figure 18.b

Figure 18: Temperature variation for different system depths, a) 600 W/m<sup>2</sup>, b) 800 W/m<sup>2</sup>.

Figure 19 shows a plan-view thermographic image after the experiment with 600 W/m<sup>2</sup> solar radiation. The colour scale varies from blue at lower temperature and increasing with rainbow colours reaching the maximum temperature at the red colour. From this figure, it is clear that reducing the depth of zeolite reduced the cooling effect hence increasing the temperature of the plate. This phenomenon occurred because there is no enough medium to gain the heat and dissipate it, so it accumulates over the plate itself.

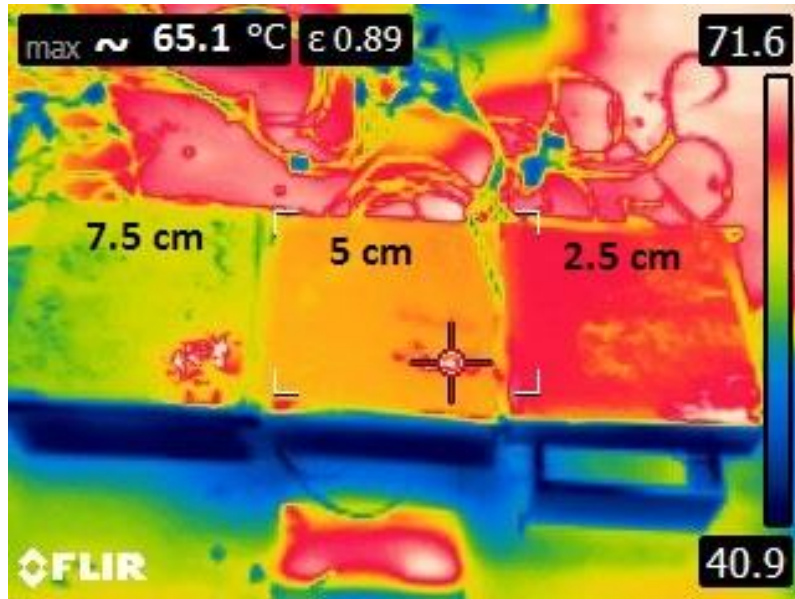


Figure 19: Temperature distribution for different depths of 7.5, 5 and 2.5 cm.

In Figure 20.a and 20.b which represent electrical efficiency variations at different depths and at different radiations, the systems showed improvement in expected efficiency, with the maximum improvement obtained using 10 cm depth with fins and metal mesh cuts/particles.

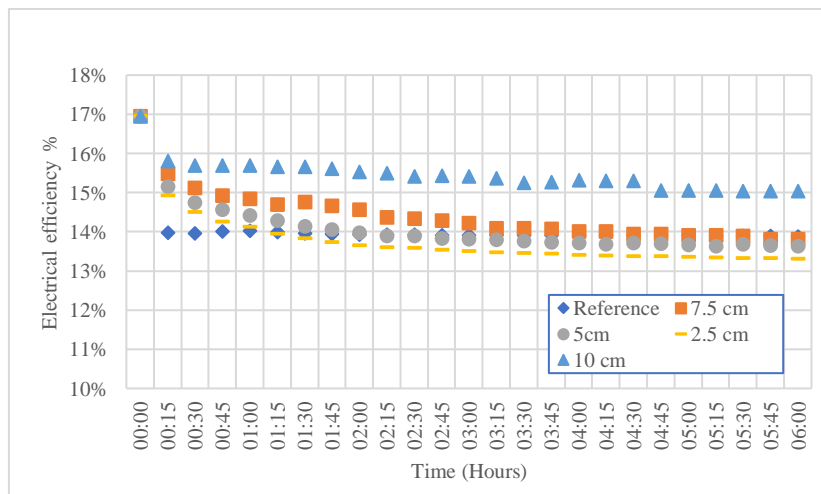


Figure 20.a

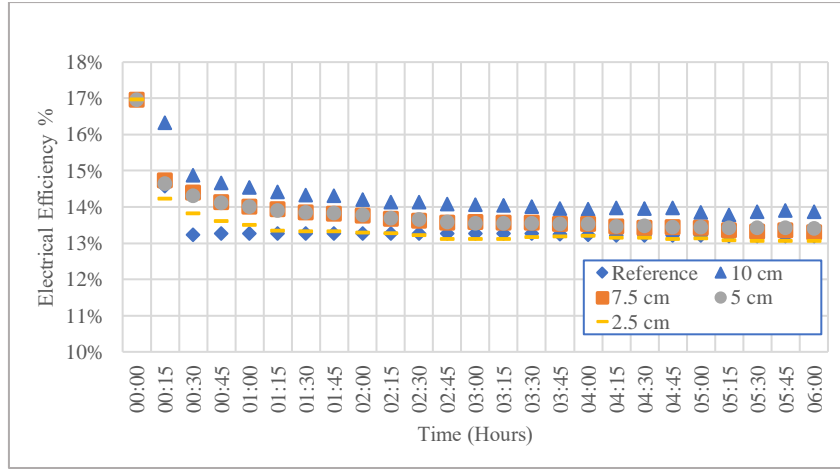


Figure 20.b

Figure 20: Electrical efficiency variation with time at different depths a. 600 W/m<sup>2</sup> b. 800 W/m<sup>2</sup>

Table 2 summarises the resultant temperature reduction and expected electrical efficiency improvement obtained from experiments with different configuration under different radiations. Average temperature reduction was calculated using the following formula:

$$\Delta T_{avg} = \frac{\sum_1^n (T_{ref} - T_c)}{N} \quad \text{Eqn.5}$$

Where:

$T_{ref}$ : The reference system temperature °C

$T_c$ : Cooled system temperature °C

N: Number of measurements

Efficiency increment was calculated at each measurement using the following formula:

$$\Delta \%_{increase} = \frac{\eta_c - \eta_{ref}}{\eta_{ref}} \% \quad \text{Eqn.6}$$

Where:

$\eta_{ref}$ : The reference system temperature °C

$\eta_c$ : Cooled system temperature °C

And the average increment over the test period was calculated using

$$\Delta \%_{avg} = \frac{\sum_1^n \Delta \%_{increase}}{N} \quad \text{Eqn.7}$$

Table2: Summary of average temperature reduction for different systems

Solar Radiation W/m <sup>2</sup>	System Configuration	Average Temperature Reduction	Average Efficiency Improvement %
600	10 cm depth + fins only	8.7 ° C	5.82%
	10 cm depth + fins + metal mesh cuts	14.9 ° C	9.93 %

	7.5 cm + fins + metal mesh cuts	4.1 ° C	2.77 %
	5 cm + fins + metal mesh cuts	0.9 ° C	0.3%
	5 cm + fins + metal mesh cuts	0 ° C	0 %
800	10 cm depth + fins only	4.1°C	2.74%
	10 cm depth + fins + metal mesh cuts	9.5 ° C	6.64%
	7.5 cm + fins + metal mesh cuts	4 ° C	2.84%
	5 cm + fins + metal mesh cuts	2 ° C	2.94%
	5 cm + fins + metal mesh cuts	0 ° C	0%
1000	10 cm depth no additives	2 ° C	1%
	10 cm depth + fins only	4.9 ° C	3.45%
	10 cm depth + fins + metal mesh cuts	8.9 ° C	6.5%

From the table above, it is clear that the proposed system significantly reduced the temperature during the test hours.

For Zeolite regeneration (re-saturation), either water submerging container below the system to saturate zeolite over night or a saturation system with water closed loop circulation can be used.

The proposed system was able to maintain the temperature of the cooled system by (9-14.9) °C below the un-cooled system which is a promising performance compared to other passive cooling systems. Table 3 shows comparison between the proposed system and other passive systems in the literature at the same metrological conditions.

Table 3: comparison between the proposed system and other passive systems.

System	Advantages	Disadvantage
Proposed system	<ul style="list-style-type: none"> <li>- Temperature reduction 9-14.9°C.</li> <li>- Zeolite availability and price.</li> <li>- System simplicity for manufacturing</li> <li>- Ability for reuse the stored heat in it (future investigation)</li> <li>- Can use saline water for cooling and the removed heat has two end uses (desalination and water heating).</li> <li>- Non-flammable and non-toxic materials used.</li> <li>- Suitable for high temperature environments.</li> </ul>	<ul style="list-style-type: none"> <li>- Higher weight compared to the fins-only systems.</li> <li>- Bad thermal conductivity of the pure zeolite</li> </ul>
PCM [29-32]	<ul style="list-style-type: none"> <li>- Temperature reduction 3-10 °C</li> <li>- Availability of different types of PCMs</li> </ul>	<ul style="list-style-type: none"> <li>- Developing technology</li> <li>- Higher initial cost.</li> <li>- Heavy weight</li> </ul>



	<ul style="list-style-type: none"> <li>- No direct contact between the panels and the cooling medium</li> <li>- Heat storage for night usage.</li> </ul>	<ul style="list-style-type: none"> <li>- Subcooling of organic PCMs</li> <li>- Bad thermal conductivity</li> </ul>
Heat pipes [33]	<ul style="list-style-type: none"> <li>- Used for concentrated solar panels</li> <li>- Various liquids can be used</li> <li>- Many end use applications</li> <li>- No power consumption</li> </ul>	<ul style="list-style-type: none"> <li>- Developing technology</li> <li>- Not simple to manufacture</li> <li>- Leakage risk</li> <li>- Higher initial cost</li> <li>- Maintenance problem</li> <li>- Heavy weight</li> </ul>
Fins cooling [34]	<ul style="list-style-type: none"> <li>- Low initial cost</li> <li>- Availability of conductive materials</li> <li>- Temperature reduction 3-8° C for natural convection</li> </ul>	<ul style="list-style-type: none"> <li>- Suitable only for cold climates.</li> <li>- Dust accumulation.</li> <li>- Not many end-uses for extracted heat.</li> <li>- Heat extracted cannot be stored.</li> </ul>

Further investigation for other absorbent material, usage of saline water, different system configuration, outdoor test experiments, thermal energy efficiency and exergy analysis with economic analysis are promising extended work on this field of research.

## 6. Conclusions

Saturated activated alumina (Zeolite) was tested as a cooling agent for solar panels under different solar radiations at same metrological conditions. Four phases of experiments were held to study different system design aspects affecting the system performance. Firstly, saturated zeolite with 10 cm depth at 1000 W/m<sup>2</sup> solar radiation and compared with uncooled system. Then, two fins were inserted to enhance the system thermal performance and heat transfer. The third phase included adding 1% wt. metal mesh cuts/particles to fill the gaps and enhanced the system performance. Finally, the effect of different depths was studied using four different depths of 2.5, 5, 7.5, and 10 cm on the system performance.

Results showed that, saturated zeolite with 10 cm depth with fins and metal mesh cuts can maintain the temperature of the system at (9 to 14.9) °C below the reference system depending on radiation intensity. The electrical efficiency was also increased with an average value of (6.5 to 10)% compared with the reference one depending on the radiation intensity as well.

## Acknowledgement

This work was supported by University of Bristol research group and Egyptian Cultural and Educational Bureau in London.

## References

- [1] <https://www.bp.com/en/global/corporate/energy-economics/statistical-review-of-world-energy.html>, last viewed 18-April-2019.
- [2] PiyushChoudhary, Rakesh Kumar Srivastava, "Sustainability perspectives- a review for solar photovoltaic trends and growth opportunities", Journal of Cleaner Production Volume 227, 1 August 2019, Pages 589-612

- [3] Idris K.Popoola, Mohammed A.Gondal, Talal F.Qahtan, Recent progress in flexible perovskite solar cells: Materials, mechanical tolerance and stability Renewable and Sustainable Energy Reviews, Volume 82, Part 3, February 2018, Pages 3127-3151
- [4] <https://news.energysage.com/what-are-the-most-efficient-solar-panels-on-the-market/>, last viewed 23- March-2019.
- [5] <https://www.civicsolar.com/support/installer/articles/how-does-heat-affect-solar-panel-efficiencies/> last viewed 23-March 2019.
- [6] M.C, Kumar S.R, and Valavan. D, "A review on the thermal regulation techniques for non integrated flat PV modules mounted on building top". Energy and Buildings 86 (2015) 692–697.
- [7] Nabil A. S Elminshawy, A.M.I. Mohamed, K. Morad, Y. Elhenawy, Abdulrahman A. Alrobaian, "Performance of PV panel coupled with geothermal air cooling system subjected to hot climatic" Applied Thermal Engineering, Volume 148, 5 February 2019, Pages 1-9.
- [8] Krauter S, "Increased electrical yield via water flow over the front of photo-voltaic panels", Solar Energy Materials and Solar Panels 82 (2004) 131–137.
- [9] Abdolzadeh M and Ameri M. "Improving the effectiveness of a photovoltaic water pumping system by spraying water over the front of photovoltaic panels" Renewable Energy 34 (2009) 91–96.
- [10] Saber Ragab Abdallah, I.M.M. ElSemary, A.A. Altohamy, M.A Abdelrahman, A.A.A. Attia, O. Ezzat Abdelatif, Experimental investigation on the Effect of Using Nanofluid (Al<sub>2</sub>O<sub>3</sub> - Water) on the Performance of PV/T System, Thermal Science and Engineering Progress (2018).
- [11] H. Fayaz, R. Nasrin, N.A. Rahim, M. Hasanuzzaman, " Energy and exergy analysis of the PVT system: Effect of Nanofluid flow rate" Solar Energy 169 (2018) 217–230.
- [12] Saber Ragab, Hind Saidani-Scott, Osama Ezzat Abdellatif, "Performance analysis for hybrid PV/T system using low concentration MWCNT (water-based) nanofluid" Solar Energy Volume 181, 15 March 2019, Pages 108-115
- [13] Mohamed Emam and Mahmoud Ahmed, Cooling concentrator photovoltaic systems using various configurations of phase-change material heat sinks, Energy conversion and Management 158 (2018) 298–314, <https://doi.org/10.1016/j.enconman.2017.12.077>.
- [14] A. Karthick, K. Kalidasa Murugavel , P. Ramanan, Performance enhancement of a building-integrated photovoltaic module using phase change material, Energy 142 (2018) 803e812, <https://doi.org/10.1016/j.energy.2017.10.090>.
- [15] M. Emam, Shinichi Ookawara, Mahmoud Ahmed, Performance study and analysis of an inclined concentrated photovoltaic-phase change material system, Solar Energy 150 (2017) 229–245.
- [16] Mawufemo Modjinou, Jie Ji, Weiqi Yuan, Fan Zhou, Sarah Holliday, Adeel Waqas, Xudong Zhao, "Performance comparison of encapsulated PCM PV/T, microchannel heat pipe PV/T and conventional PV/T systems", Energy, Volume 166, 1 January 2019, Pages 1249-1266.
- [17] Daisuke Sato, Noboru Yamada, Review of photovoltaic module cooling methods and performance evaluation of the radiative cooling method, Renewable and Sustainable Energy Reviews Volume 104, April 2019, Pages 151-166.

- [18] Bahaidarah HMS, Baloch AAB, Gandhidasan P. Uniform cooling of photovoltaic panels: a review. *Renew Sustain Energy Rev* 2016;57:1520–44.
- [19] Mittelman, G., Alshare, A., Davidson, J.H., 2009. A model and heat transfer correlation for rooftop integrated photovoltaics with a passive air cooling channel. *Sol. Energy* 83, 1150–1160. doi:10.1016/j.solener.2009.01.015
- [20] Jubayer, C., Siddiqui, K., Hangan, H., 2016. CFD analysis of convective heat transfer from ground mounted solar panels. *Sol. Energy* 133, 556–566. doi.org/10.1016/j.solener.2016.04.027
- [21] [https://www.engineeringtoolbox.com/water-thermal-properties-d\\_162.html](https://www.engineeringtoolbox.com/water-thermal-properties-d_162.html), last viewed 23- March-2019.
- [22] <https://www.drytechinc.com/why-silica-gel-breathers-just-dont-cut-it/> last viewed 23- March- 2019.
- [23] Marco Simonetti, Vincenzo Gentile, Gian Vincenzo Fracastoro, Angelo Freni, Luigi Calabrese, Giacomo Chiesa, ‘Experimental testing of the buoyant functioning of a coil coated with SAPO34 zeolite, designed for solar DEC (Desiccant Evaporative Cooling) systems of buildings with natural ventilation, *Applied Thermal Engineering*, Volume 103, 25 June 2016, Pages 781–789
- [24] Iverola, A., Mellor, A., Alonso Alvarez, D., Ferre Llin, L., Guarracino, I., Markides, C.N., Paul, D.J., Chemisana, D. and Ekins-Daukes, N. (2018) Mid-infrared emissivity of crystalline silicon solar cells. *Solar Energy Materials and Solar Cells*, 174, pp. 607–615.
- [25] 2009 ASHRAE Handbook: Fundamentals - IP Edition. Atlanta: American Society of Heating, Refrigerating and Air-Conditioning Engineers. 2009. ISBN 978-1-933742-56-4.
- [26] J. Jeon, S. Park, B. J. Lee Analysis on the performance of a flat-plate volumetric solar collector using blended plasmonic nanofluid, *Solar Energy*, Volume 132, July 2016, Pages 247–256.
- [27] Evans D.L, "Simplified method for predicting photovoltaic array output". *Solar Energy*, Vol. 27, PP. 555–560, (1981).
- [28] Holman JP. *Experimental methods for engineers*. New York: McGraw-Hill;2012.
- [29] Indartono SY, Suwono A, Fendy Yuseva Pratama. Improving photovoltaics performance by using yellow petroleum jelly as phase change material. *Low Carbon Technol* 2014;10:1093–9.
- [30] Hasan A, Alnoman H, Rashid Y. Impact of integrated photovoltaic-phase change material system on building energy efficiency in hot climate. *Energy Build* 2016;130:495–505. <http://dx.doi.org/10.1016/j.enbuild.2016.08.059>
- [31] Hasan A, Sarwar J, Alnoman H, Abdelbaqi S. Yearly energy performance of a photovoltaic-phase change material (PV-PCM) system in hot climate. *Sol Energy* 2017;146:417–29. <http://dx.doi.org/10.1016/j.solener.2017.01.070>.
- [32] Hachem F, Abdulhay B, Ramadan M, El Hage H, El Rab MG, Khaled M. Improving the performance of photovoltaic cells using pure and combined phase change materials – experiments and transient energy balance. *Renew Energy* 2017;107:567–75. <http://dx.doi.org/10.1016/j.renene.2017.02.032>.
- [33] Darkwa JDD, Kokogiannakis JG. Thermal management systems for photovoltaics installations. *Sol Energy* 2013;97:238–54.
- [34] Juwel Chandra Mojumder, , Hwai Chyuan Ong K.Y. Leong, Abdullah-Al-Mamoona

“An experimental investigation on performance analysis of air type photovoltaic thermal collector system integrated with cooling fins design” Energy and Buildings Volume 130, 15 October 2016, Pages 272-285.